Journal homepage www.jzs.univsul.edu.iq
Journal of Zankoy Sulaimani
Part-A- (Pure and Applied Sciences)

Cr-spinel Mineral Chemistry from Sawlava Ophiolite Complex, Kurdistan, NW Iran, Geotectonic Setting Implication

Bahman Rahimzadeh[1], Fariborz Masoudi[1], Amir Ali Tabbakh Shabani[2]

[1]*Faculty of Earth Sciences, Shahid Beheshti University, Tehran, Iran*.
[2] *Faculty of Earth Sciences, Kharazmi University, Tehran, Iran.*
E-mail: B.rahimzade59@gmail.com

Article info

Original: 06.10.2015
Revised:15.05.2016
Accepted:16.06.2016
Published online: 01.07.2016

Key Words:
Cr-Spinel, Chromitite, Sawlava ophiolitic complex, Zagros, Iran

Abstract

Ophiolitic ultramafic rocks associated with chromitite lenses are studied in detail from Sawlava ophiolitic complex along the Zagros suture in the northwest of Iran. Except one small window in Miana village almost all primary silicates in dunites and wehrlites have been altered to serpentine; however, Cr-spinel is the surviving phase left. Chemistry of the Cr-spinel minerals from small chromitite lenses within the ultramafic units provides information about the primary petrological characteristics. The Cr# of the Cr-spinels is between 0.76 to 0.82 in chromitite lenses, 0.58 to 0.67 in dunite and 0.49 to 0.52 in wehrlite. Al_2O_3 values and FeO/MgO ratio in the chromitite lenses indicate a boninitic melt for the source magmas of the Cr-spinels. The low values of Ti and high contents of Al and high Cr# in peridotite Cr-spinels reveal a pronounced rate of partial melting (25-35%) for peridotites. This suggests that Sawlava complex source was mantle wedge with elevated degrees of partial melting. Olivine, clinopyroxene and Cr-spinel mineral chemistry shows the characterization similar to those in abyssal to supra-subduction zone (SSZ) peridotites which suggest a fore-arc basin setting for the generation of the chromitite lenses from Sawlava ophiolites.

Introduction

Cr-spinel chemistry is considered as an important petrogenetic indicator in peridotites [1, 2, 3 and 4]. Main minerals such as olivine and pyroxene in mafic and ultramafic rocks (especially ophiolitic peridotites) are usually altered but chromite and Cr-spinel are the only primary minerals that can be preserved even in completely serpentinized peridotites [5]. The latter two minerals are generally used to identify altered mafic and ultramafic rocks [4 and 6] and specifically Cr-spinel is the main useful mineral to understand primary petrological characteristics of highly altered ultramafic rocks [5 and 7].

Chromitite has an advantage in unraveling the alteration features of chromian spinel because of its simple chemical composition as compared with other igneous rocks, where precursor spinel may have complicated intra-grain or inter-grain chemical heterogeneity [8]. Chromitite forms in different mafic-ultramafic geologic environments such as ophiolites, Uralian-Alaskan-type complexes and stratiform or layered complexes. Podiform chromites in ophiolites are geochemically classified by many authors as either high-Al ($Al_2O_3 \geq 25\%$) or high-Cr ($Cr_2O_3 \geq 45\%$ to 60%) [9, 10].This classification reflects actually the nature of Cr-spinel parent magma [11, 12].

In this study we documented the mafic minerals and Cr-spinel composition in the chromitite, dunite and wehrlite by electron microprobe analysis to investigate petrogenetic features and geotectonic setting of Sawlava ophiolitic complex in Kurdistan, NW of Iran.

Analytical Methods

Whole-rock major and trace elements were obtained by X-ray fluorescence (XRF) technique on pressed-powder pellets, using an ARL Advent-XP automated X-ray spectrometer in Ferrara University, Rome, Italy. Calibration was made using international reference materials and the matrix correction method was applied [13]. Accuracy and detection limits were determined using international reference standards run as unknowns. Mean accuracies were generally better than 2% for major elements, and 5% for trace elements. The detection limits for trace elements were: Zn, Ba, Cu, Sc = 5 ppm; Ga, Ni, Co, Cr, V, Sr, Nb, La, Zr = 2 ppm; Rb, Y = 1 ppm. Representative analyses from different rock types are presented in Table 2.

Major element compositions of minerals were determined by electron probe micro-analysis (EPMA) technique using a Cameca Camebax instrument at the Instituto di Geoscienze e Georisorse, CNR, Padua, Italy. The acceleration voltage and probe current were 15 keV and 20 μA, respectively, and the counting time was 100 seconds. Instrumental calibration was made using natural and synthetic mineral standards. Matrix corrections were performed using the PAP method [14]. Analytical precision was better than ±2% for elements in the range of 10-20 wt% oxide, better than 5% for elements in the range 2-10 wt% oxide, and better than 10% for elements in the range of 0.5-2 wt% oxide. Representative analyses of minerals from Sawlava peridotites are presented in Table 2. Mg#, Cr#, Fe^{2+} and Fe^{3+}, $Mg/(Mg + Fe^{2+})$, $Cr/(Cr + Al)$, $Fe^{2+}/(Fe^{2+} + Mg)$ and $Fe^{3+}/(Fe^{3+} + Al + Cr)$ atomic ratios are calculated for analyzed minerals. The Fe_2O_3 and FeO were calculated from the measured total FeO according to Droop [15].

Geology

Zagros ophiolites are part of the Tethyan ophiolitic belt of the Middle East which links the eastern Mediterranean-Turkish ophiolites in the west and the Oman (Somail) ophiolites, in the south (Fig. 1). The great part of the Zagros ophiolites is related to Neo-Tethys Ocean and recorded to form in the Jurassic to Cretaceous -Paleocene. Zagros suture zone is regarded as one branch of the Neo-Tethys Ocean that extends from the border of Iran-Turkey (northwest) to Oman (south of Iran). This branch of the Neo-Tethys Ocean started opening in the Triassic period [16] and began to close in the upper Cretaceous [17] and lasted in the northwest of Zagros to the middle Eocene [18]. Kermanshah ophiolites [19] and Neyriz ophiolites [20, 21], exposed in the Zagros suture zone, are related to those ophiolites of the upper Cretaceous age. The two parallel domains of the Sanandaj-Sirjan metamorphic zone and the Urumieh-Dokhtar magmatic arc are believed to be the result of the NE-dipping subduction of the Neo-Tethys beneath the Central Iran [16].

In NE of Iraq two types of serpentinite of Jurassic and Cretaceous age crop out [22]. The Jurassic serpentinite is imbricated and the Cretaceous serpentinite-matrix is mélange. The first type, associated with ophiolite, includes serpentinite broken formation with 80-120 Ma that is similar to the Kermanshah complex [19]. The second type of serpentinite that has drastically different petrogenesis, age and regional field relationships, consists of exotic blocks of mixed ages (150-200 Ma) and possesses εNd(i) down to −30 [22].

Based on the chemical compositions and initial isotope ratios of $^{87}Sr/^{86}Sr$ and $^{143}Nd/^{144}Nd$, [23] concluded that basaltic and gabbroic bodies along the NW of the Zagros fault originated from a depleted mantle in the Cenozoic implying that the Kurdistan complex was part of the supra-subduction zone (SSZ) ophiolite, cropping out in the collision of the Arabian and Iranian plates probably in the Miocene or later.

Our study ophiolitic complex is located in the north and north east of Sawlava town, between Sanandaj and Marivan cities (Fig. 2). Geologically, the ophiolitic complex crops out along the Zagros thrust between Sanandaj-Sirjan and High Zagros structural zones. Sawlava ophiolitic rocks consist of large units of volcanic rocks with minor intrusive sequences. Pillow lava, microgabbro, pegmatitic gabbro and gabbro are the main rock units. Ultramafic rocks such as brecciated-serpentinized dunite and wehrlite are also present (Fig. 2). In few locations such as Vaise and Sianav Villages in the west of the study area, outcropped chromitite is covered by serpentinite in several places. Chromitites form small (<1 m in thickness) pods with irregular to lenticular shapes. Neither layering nor graded bedding is observed within the pods.

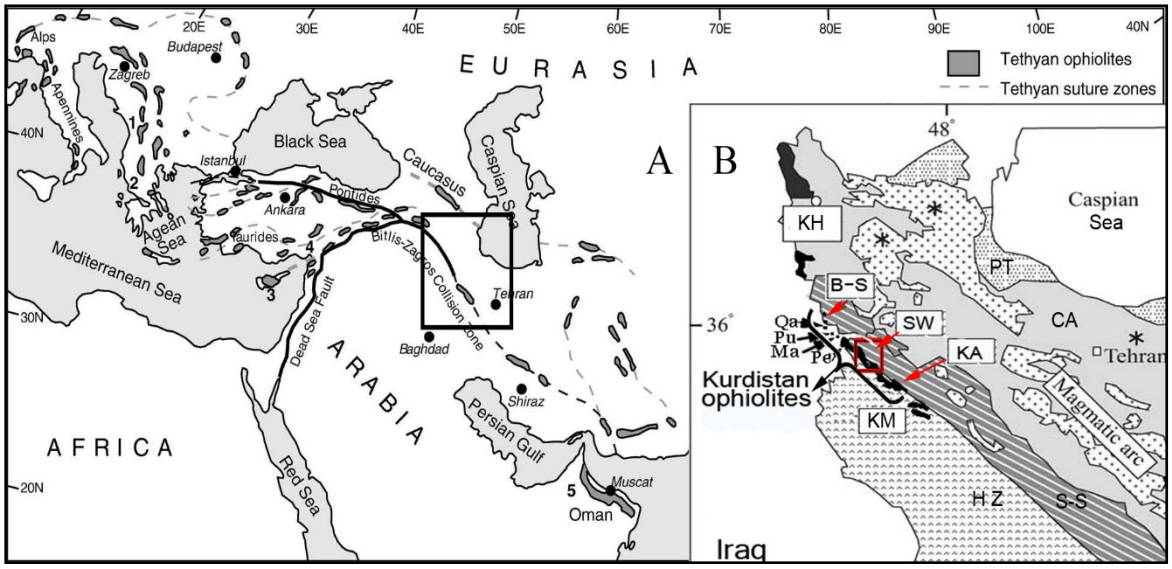

Fig. 1.A: The location of Kurdistan ophiolitic complex in the main ophiolite belts along the Tethyan suture [24] B: A close up of the rectangle in A, shows NW of Iran displaying the main geological formations, (Modified after [25]. (HZ: High Zagros zone (Zagros Folded Thrust Belt [26]); S-S: Sanandaj-Sirjan zone; CA: Central Iran zone; PT: Paratethys basin; KM: Kermanshah ophiolite; KH: Khoy ophiolite and Kurdistan ophiolite complex (B-S: Bane-Sardasht; SW: Sawlava; KA: Kamiaran; Qa: Qalandar sepentinite; Pa: Pauza ultramafic rocks; Ma: Mawat; Pe: Penjwin). The study area is shown by a quadrangle.

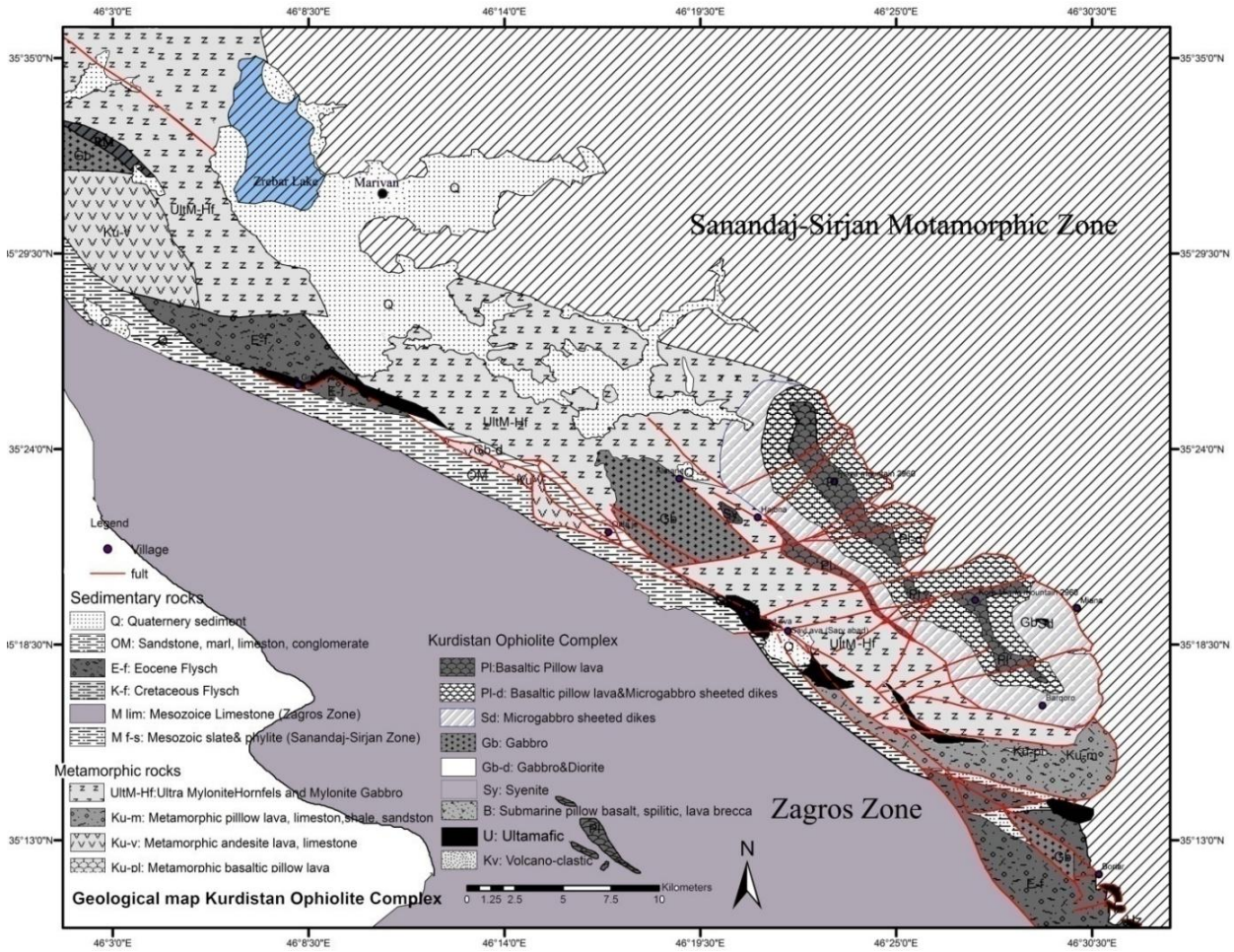

Fig. 2. Geological map of the Kurdistan ophiolite, modified after [27].

Petrography

In the Sawlava ophiolites along the Zagros thrust, except a window in the east of the area, almost all peridiotites altered to serpentininte and the main minerals such an olivine and pyroxene are not preserved. However, in small outcrop of fresh dunite and wehrlite, euhedral to subhedral olivine with Mg# (FO=88-92) makes up 95% of dunite and about 85% of wehrlite. Anhedral clinopyroxenes (diopside-clinoenstatite) fill the spaces between olivine crystals to form cumulate texture; Cr-spinel and magnetite are accessory minerals in these rocks. The part of peridotite, adjacent to the Zagros thrust, altered to serpentinite showing mesh texture and consists mainly of chrysotile/antigorite. In general, Cr-spinel and magnetite comprise <1 to 5% of dunite, wehrlite and serpentinite.

Chromitite occurs as pods mostly <1 m across within strongly sheared serpentinites. Fresh primary silicates, olivine and clinopyroxene are enclosed as minute globular mono mineral inclusions within Cr-spinel grains (fig. 3- A). The silicate minerals in Cr-spinel grains are almost altered to serpentine and calcite. Secondary calcite fills the fractures of chromitite as well. Main minerals and textures of Sawlava rock units are summarized in Table 1.

Table 1. A summary of mineralogy and petrography of ultramafic rocks in Sawlava ophiolites. (Ol: Olivine; Cpx: Clinopyroxene; Chr-Spl: Chromian-Spinel; Mag: Magnetite; Ctl: Chrysotile; Atg: Antigorite; Srp: Serpentine; Cal: Calcite; Tlc: Talc; Chl: Chlorite; Ser: sericite) (Abbreviations from [28]. outcrop percents are based on field observations.

rocks name	*texture*	*main minerals in order*	*secondary minerals*	*outcrop in complex*
dunite	*granular*	*Ol, Chr-Spl, Cpx*	*Srp, Cal, Tal, Chl*	*10%*
wehrlite	*cumulate*	*Ol, Cpx, Chr-Spl*	*Srp, Chl, Tal, Ser*	*10%*
serpentinite	*mesh, fibrous*	*Ctl, Atg, Chr-Spl*	*Cal, Tlc, Chl*	*79%*
chromitite	*granular*	*Chr-Spl, Mag, Ol, Cpx,*	*Srp, Cal, Chl*	*1%*

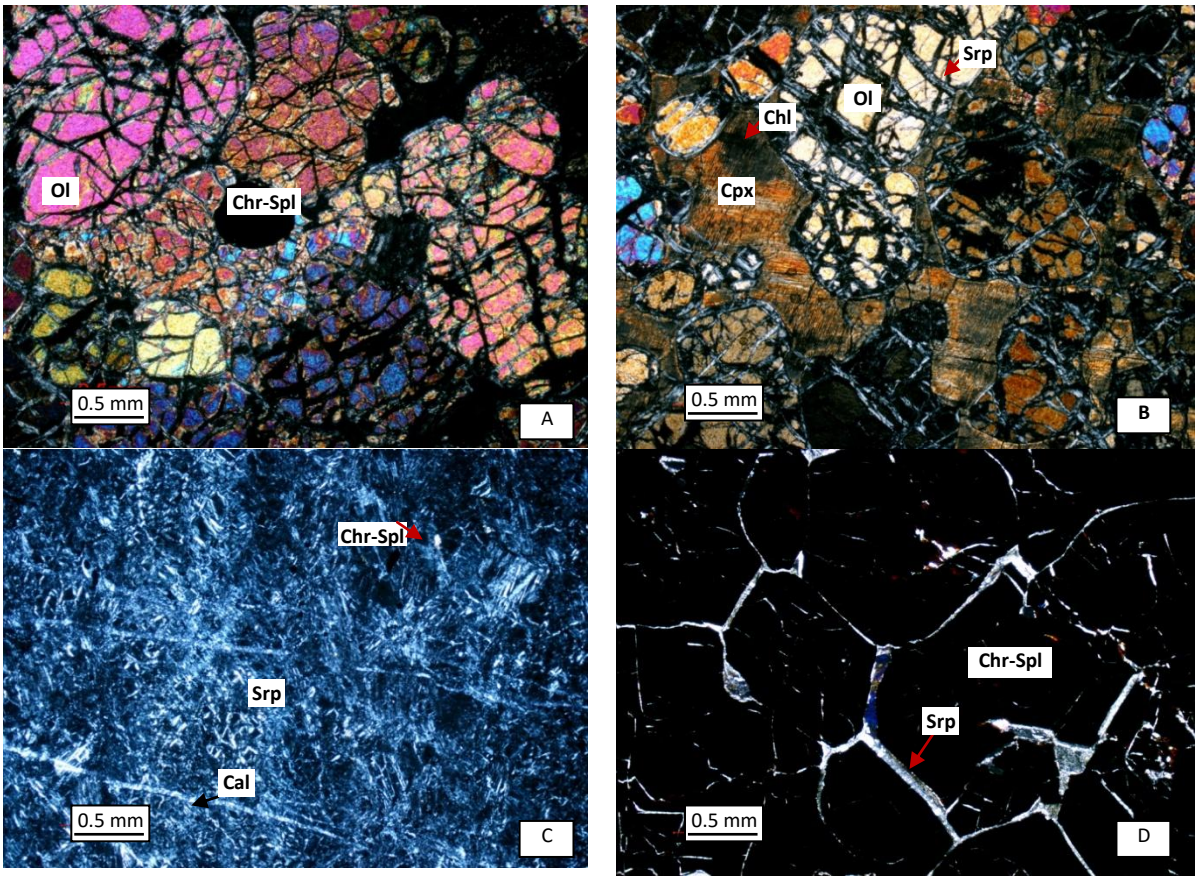

Fig. 3. Photomicrographs of Cr-spinel in dunite, wehrlite and chromitite from Sawlava ophiolite. A) subhedral olivine (Ol) showing mesh texture and Cr-spinel (Chr-Spl) in dunite. Along the fractures olivine altered to serpentine (Srp) (Q42). B) anhedral clinopyroxene (Cpx) fills the spaces between the subhedral olivine displaying mesh texture in wehrlite. Olivine altered to serpentine and clinopyroxene altered to sericite and chlorite (Chl) (Q43). C) A serpentinite

enclosing Cr-spinels and calcite veins resulted from the complete alteration of ultramafic rocks (R11). D) Serpentine fills the grain boundaries of euhedral Cr-spinel in chromitite (P27). (All microscopic photos are taken in XPL).

Whole rock chemistry

Analyses of six representative whole rock samples of the peridotites and one sample of chromitite from the Sawlava area are presented in Table 2. The SiO_2 contents of the peridotites range from 42.50 to 45.68 wt%. All Fe is assumed to be ferrous in peridotite; however, Fe_2O_3 and FeO are calculated for chromitite. The analyzed samples are rich in MgO (40.88-46.35wt %), with a wide range in concentration of Al_2O_3 (0.89-3.09wt %), CaO (0.10-1.13wt %) and TiO_2 (0.02-0.13wt %). Al_2O_3 is expected to be the most immobile major element in serpentinized peridotites [29] CaO is correlated with clinopyroxene abundances [30], as clinopyroxene is the main CaO-bearing phase in these rocks. Therefore, the low amounts of CaO and Al_2O_3 in Sawlava peridotites show low contents of clinopyroxene in the original samples. Higher amounts of LOI in some peridotite samples are attributed to the extensive serpentinization. Based on petrography and geochemistry data (Table 2) the Q labeled samples most likely represent cumulitic peridotites rather than mantle peridotites. Chromitite possess high value of Cr_2O_3 (50.15 wt %) that places this sample in the high chromite position and very similar to Mining Camp in Oman and Mavat chromitite [31, 32]. Also the content of Al_2O_3 (10.80 wt %) sets Sawlava chromitite in the low Al position [9, 10].

Table 2 - Whole rock XRF analyses of the representative samples from Sawlava peridotites and chromitite. The values of Fe^{3+} and Fe^{2+} were calculated from the measured total FeO according to [15].

Ele	*Q-9*	*Q-12*	*Q-11*	*Q-42*	*Q-43*	*R-11*	*P-27*
Rock	*Serpentinized peridotite*			*Peridotite*		*Serpentinite*	*Chromitite*
SiO₂	*45.54*	*42.82*	*42.57*	*42.50*	*40.78*	*45.68*	*6.00*
TiO₂	*0.03*	*0.13*	*0.10*	*0.11*	*0.08*	*0.02*	*0.18*
Al₂O₃	*0.89*	*1.75*	*3.09*	*1.86*	*1.50*	*0.75*	*5.35*
FeO	*8.04*	*10.59*	*9.36*	*9.90*	*10.76*	*8.80*	*9.90*
MnO	*0.14*	*0.14*	*0.13*	*0.15*	*0.17*	*0.16*	*0.41*
MgO	*44.54*	*44.04*	*43.12*	*44.52*	*45.75*	*44.59*	*20.34*
CaO	*0.31*	*0.22*	*1.13*	*0.43*	*0.56*	*0.00*	*7.30*
Na₂O	*0.01*	*-*	*-*	*-*	*-*	*-*	*-*
P₂O₅	*-*	*-*	*-*	*0.01*	*-*	*-*	*-*
Total	*99.55*	*99.61*	*99.47*	*99.49*	*99.53*	*100.02*	*49.52*
Cr	*2393*	*1621*	*1313*	*1918*	*1685*	*2686*	*343100*
LOI	*10.07*	*11.51*	*11.61*	*7.28*	*7.66*	*12.35*	*4.98*
Ni	*2663*	*1885*	*2172*	*1802*	*1769*	*1951*	*285*
Zr	*4*	*9*	*6*	*3.5*	*1.7*	*-*	*38*
Sr	*6*	*7*	*8*	*6*	*9*	*2*	*33*
Th	*-*	*-*	*-*	*0*	*0*	*-*	*1*
V	*42*	*42*	*32*	*43*	*30*	*54*	*930*
S			*74*	*-*	*-*	*8*	*8*
Zn	*35*	*44*	*41*	*55*	*51*	*38*	
Cu	*6*	*34*	*24*	*29*	*11*	*4*	*4*
Sc	*6*	*5*	*2*	*-*	*0.2*	*7*	*7*
Co	*106*	*95*	*93*	*114*	*99.4*	*111*	*52*
Y		*3*	*2*	*-*	*-*	*-*	*-*
Pb	*-*	*-*	*-*	*0..5*	*0..5*	*0.4*	*0.4*

Variations of selected oxides in Sawlava peridotites are shown in binary diagrams in terms of SiO_2, Al_2O_3, FeO, and CaO versus MgO (Fig.4). The composition of primitive mantle [33] is also included in the variation diagrams for comparison. SiO_2 content of Sawlava ophiolites is relatively similar to primitive mantle. The positive correlation of FeO with MgO may reflect the influence of cumulate processes involving crystallization of relatively Fe-rich olivine [34] (Fig. 4).

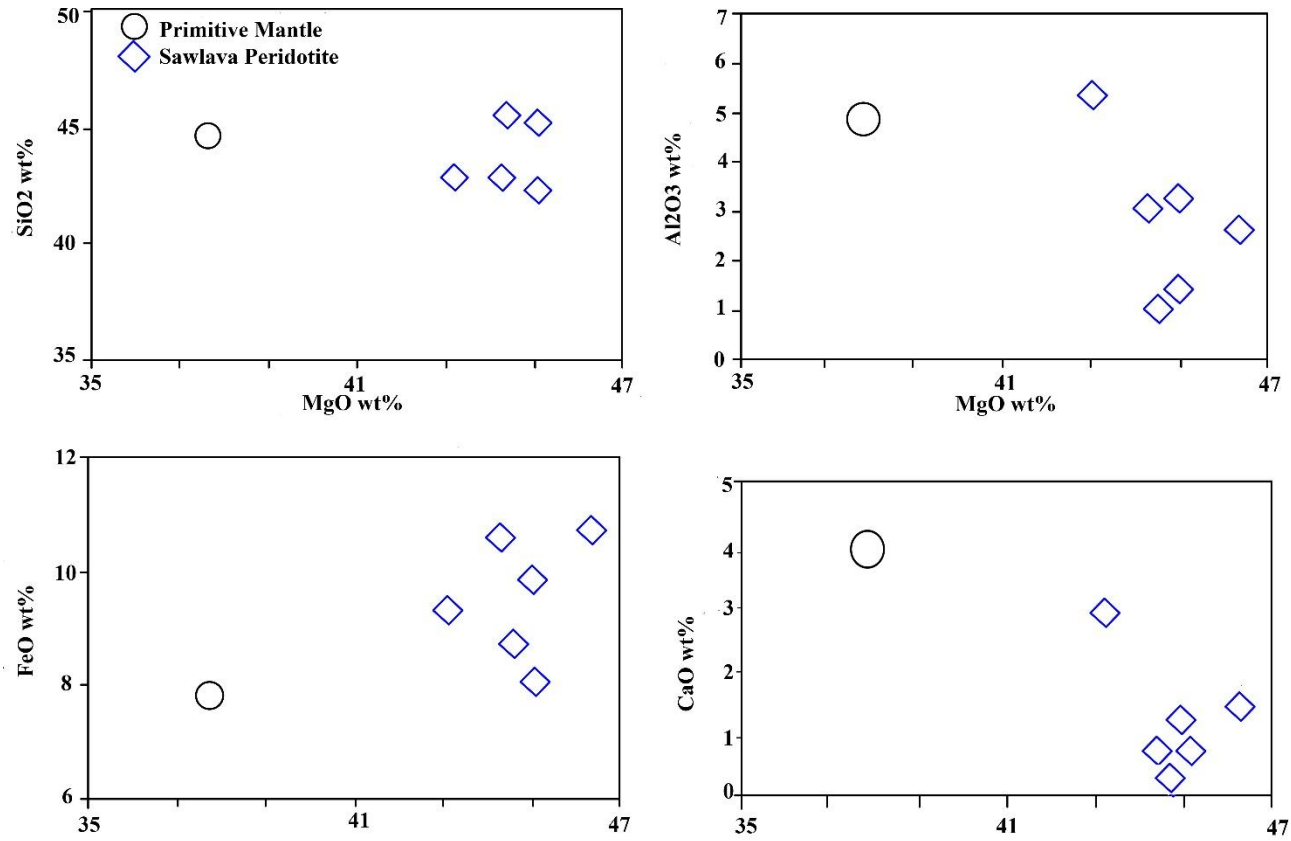

Fig. 4 - Variation diagrams of Al_2O_3, CaO, SiO_2 and FeO versus MgO in peridotites of Sawlava ophiolite. The composition of primitive mantle [33] is included for comparison.

Mineral chemistry

Cr-spinel

Cr-spinel grains in chromitite and peridotite are homogenous in composition and lack any zoning. Cr-number of Cr-spinel grains in chromitite, dunite and wehrlite ranges from 0.76 to 0.82, 0.58 to 0.68 and 0.49 to 0.52 respectively. In overall, it is found that Cr# of chromitite> Cr# of dunite >Cr# of wehrlite and Mg# of chromitite< Mg# of dunite < Mg# of wehrlite (Table 3). Negative correlation between Cr# and Mg# reflects the unequal partition coefficients of Mg and Fe between chromite and olivine during crystallization process [2]. With respect to chromite crystallization process in magma, Fe distinctively enters into the chromite phase, whereas, Mg accommodates in the olivine crystal structure. The relationship between Mg# and Cr# is a common trait for all ophiolitic chromitites [9]. TiO_2 contents in Cr-spinel from chromitite and wehrlite range from 0.08-0.18 and 0.06-0.13 wt%, respectively; however, two different ranges of TiO_2 (0.95-0.99 and 2.19-4.24) are present in dunite samples.

Olivine

Olivine crystals in dunite and wehrlite have forsterite content ranging from 88% to 91% (Mg#=0.88-0.91). The olivine composition can be represented as $(Mg_{(0.88\text{-}0.91)}, Fe_{(0.12\text{-}0.09)})_2 SiO_4$ that is between forsterite to hortonolite. It is generally homogenous without distinctive zoning and its crystals represent low CaO (< 0.2 wt. %), and MnO (< 0.2 wt. %); furthermore, its NiO contents in wehrlite and dunite are similar (Table 4).

Pyroxene

All clinopyroxene crystals in the study peridotites are unzoned and can be grouped into two types of augite with $En_{(49.4\text{-}55.9)}Wo_{(36.4\text{-}44.2)}$ $Fs_{(4.7\text{-}6.7)}$ composition and Mg#=0.64-0.89; clino-enstatite with $En_{(91.99\text{-}93.94)}Wo_{(2.16\text{-}3.8)}$ $Fs_{(3.78\text{-}3.82)}$ and Mg#=96.01-96.13. As Mg# is decreasing, TiO_2 and Na_2O contents in clinopyroxene from peridotites are increasing gradually. Clino-enstatite is in the form of exsolution blades

that wrought between diopside-augite solid solution. FeO, CaO and TiO_2 values in diopside-augite range from 3.03-4.29 wt. %, 18 - 22 wt. % and 0.32-0.84 wt. %, respectively (Table 5).

Table 3. 1. Representative microanalyses of the Cr-spinel along with their structural formulas based on 6 oxygen atoms from Sawlava ophiolites chromitite.

	P27					P28			P28- 3		P20		P20- 2	
Elem	**1**	**2**	**3**	**4**	**5**	**1**	**2**	**1-core**	**2-mid**	**3-rim**	**1**	**2-rim**	**2-mid**	**2core**
SiO_2	0.14	0.07	0.07	0.08	0.11	1.00	0.04	0.35	0.15	2.73	1.50	1.84	1.23	0.82
TiO_2	0.17	0.16	0.19	0.18	0.13	0.14	0.14	0.08	0.16	0.11	0.14	0.12	0.14	0.13
Al_2O_3	11.27	11.08	11.52	11.39	10.95	9.49	9.67	7.68	9.27	7.36	9.35	8.86	8.82	9.41
Cr_2O_3	56.27	56.36	56.31	56.73	56.32	54.15	54.26	52.43	55.29	49.19	55.31	51.68	53.27	53.59
Fe_2O_3	4.43	4.59	4.31	4.43	5.03	5.85	7.06	9.63	6.67	9.28	3.33	7.82	7.03	6.09
FeO	16.83	16.71	16.95	17.26	16.42	16.61	16.56	12.13	16.38	10.85	19.28	14.31	15.98	16.76
MnO	0.34	0.32	0.31	0.21	0.31	0.20	0.12	0.15	0.17	0.17	0.25	0.28	0.27	0.28
MgO	11.36	11.11	11.13	11.02	11.36	11.64	10.83	13.03	11.09	16.02	10.41	13.58	12.06	11.14
CaO	0.00	0.03	0.02	0.05	0.04	0.16	0.14	3.70	0.16	2.26	0.09	0.01	0.34	1.11
V_2O_5	0.00	0.00	0.00	0.00	0.00	0.29	0.27	0.27	0.28	0.24	0.32	0.21	0.30	0.25
NiO	0.12	0.09	0.07	0.07	0.06	0.09	0.10	0.08	0.09	0.90	0.08	0.09	0.09	0.07
ZnO	0.00	0.00	0.00	0.00	0.00	0.04	0.07	0.05	0.02	0.06	0.06	0.08	0.06	0.08
Total	100.5	100.0	100.45	100.3	100.22	100.19	99.97	99.99	99.97	100.50	99.77	99.01	100.01	99.99
Si	0.004	0.002	0.002	0.003	0.004	0.033	0.001	0.012	0.005	0.09	0.002	0.060	0.041	0.027
Ti	0.004	0.004	0.005	0.004	0.003	0.003	0.004	0.002	0.004	0.003	0.004	0.003	0.003	0.003
Al	0.427	0.425	0.440	0.433	0.419	0.370	0.381	0.309	0.363	0.286	0.371	0.341	0.344	0.37
Cr	1.449	1.450	1.441	1.446	1.445	1.415	1.432	1.414	1.454	1.297	1.471	1.336	1.393	1.414
Fe3	0.107	0.112	0.105	0.107	0.123	0.142	0.177	0.249	0.165	0.231	0.152	0.196	0.175	0.154
Fe2	0.452	0.455	0.459	0.465	0.445	0.463	0.466	0.344	0.459	0.304	0.482	0.388	0.445	0.471
Mn	0.009	0.009	0.008	0.009	0.008	0.00	0.00	0.00	0.00	0.00	0.00	0.00	0.00	0.00
Mg	0.544	0.539	0.537	0.530	0.550	0.574	0.539	0.67	0.55	0.789	0.522	0.676	0.599	0.559
Ca	0.000	0.001	0.001	0.002	0.002	0.00	0.00	0.00	0.00	0.00	0.00	0.00	0.00	0.00
Ni	0.003	0.002	0.002	0.002	0.002	0.00	0.00	0.00	0.00	0.00	0.00	0.00	0.00	0.00
Tot. cat.	3.000	3.000	3.000	3.000	3.000	3.000	3.000	3.000	3.000	3.000	3.000	3.000	3.000	3.000
Cr#	0.773	0.773	0.766	0.770	0.775	0.793	0.790	0.821	0.800	0.819	0.799	0.797	0.802	0.793
Fe_2#	0.454	0.458	0.461	0.468	0.448	0.446	0.464	0.339	0.455	0.278	0.480	0.365	0.426	0.457
Mg#	0.546	0.542	0.539	0.532	0.552	0.554	0.536	0.661	0.545	0.722	0.520	0.635	0.574	0.543
Fe_3#	0.054	0.056	0.052	0.054	0.0618	0.073	0.088	0.1262	0.0832	0.1273	0.05	0.1046	0.0915	0.079
Cr+Al	1.876	1.875	1.881	1.879	1.864	1.785	1.813	1.723	1.817	1.583	1.842	1.677	1.737	1.784

Table 3.2. Representative microanalyses of the Cr-spinel with their structural formulas based on 6 oxygen atoms from dunites of Sawlava ophiolites.

	Q11			Q42-4			Q42-3			Q12				
Elem	**1**	**2**	**3**	**1**	**2**	**3**	**1**	**2**	**3**	**1**	**2**	**3**	**4**	**5**
SiO_2	0.10	0.39	0.00	0.05	0.10	0.13	0.09	0.07	0.15	0.05	0.13	0.17	0.06	0.02
TiO_2	3.43	3.52	2.19	0.98	0.95	0.99	3.90	4.24	3.33	3.17	3.01	2.72	3.56	3.27
Al_2O_3	16.29	14.58	19.65	18.90	19.79	19.54	14.03	12.52	13.09	14.88	15.07	17.08	14.25	15.12
Cr_2O_3	42.04	40.27	41.16	44.47	43.55	43.89	41.60	41.24	41.43	42.83	42.99	43.39	40.53	42.05
Fe_2O_3	8.72	10.10	9.17	7.74	7.65	7.48	9.69	10.78	11.62	8.78	8.82	6.24	10.70	9.79
FeO	16.11	19.52	14.22	13.52	13.79	13.93	18.64	18.43	18.40	18.15	17.26	18.53	20.17	18.35
Mno	0.31	0.24	0.28	0.25	0.27	0.27	0.25	0.33	0.32	0.30	0.31	0.52	1.10	0.30
MgO	14.12	11.82	14.09	14.46	14.41	14.34	12.32	12.28	12.53	12.24	12.81	12.02	10.66	12.33
CaO	0.00	0.02	0.01	0.01	0.00	0.02	0.00	0.00	0.00	0.00	0.04	0.05	0.04	0.01
NiO	0.19	0.28	0.21	0.16	0.20	0.18	0.31	0.34	0.22	0.23	0.19	0.11	0.24	0.26
Total	100.44	99.73	100.07	99.77	99.95	100.00	99.86	99.14	99.91	99.75	99.75	100.21	100.23	100.42
Si	0.003	0.012	0.000	0.002	0.003	0.004	0.003	0.002	0.005	0.001	0.004	0.005	0.002	0.001
Ti	0.080	0.084	0.050	0.023	0.022	0.023	0.093	0.103	0.081	0.076	0.072	0.064	0.086	0.077
Al	0.604	0.548	0.705	0.687	0.716	0.707	0.527	0.476	0.498	0.558	0.562	0.633	0.538	0.560
Cr	1.027	1.016	0.986	1.084	1.057	1.066	1.048	1.052	1.048	1.077	1.076	1.079	1.028	1.053
Fe_3	0.203	0.242	0.209	0.180	0.177	0.173	0.232	0.262	0.282	0.210	0.210	0.148	0.258	0.231
Fe_2	0.419	0.521	0.360	0.349	0.354	0.358	0.497	0.497	0.497	0.483	0.457	0.488	0.541	0.485
Mn	0.008	0.006	0.007	0.007	0.007	0.007	0.007	0.009	0.009	0.008	0.008	0.014	0.030	0.008
Mg	0.651	0.562	0.677	0.665	0.659	0.657	0.585	0.590	0.574	0.580	0.604	0.564	0.510	0.578
Ca	0.000	0.001	0.000	0.000	0.000	0.001	0.000	0.000	0.000	0.000	0.001	0.002	0.001	0.000
Ni	0.005	0.007	0.005	0.004	0.005	0.004	0.008	0.009	0.006	0.006	0.005	0.003	0.006	0.007
Tot. cat.	3.000	3.000	3.000	3.000	3.000	3.000	3.000	3.000	3.000	3.000	3.000	3.000	3.000	3.000
Cr#	0.630	0.649	0.583	0.612	0.596	0.601	0.665	0.688	0.678	0.659	0.657	0.630	0.656	0.653
Fe^{+2}#	0.392	0.481	0.347	0.344	0.349	0.353	0.459	0.457	0.464	0.454	0.430	0.464	0.515	0.456
Mg#	0.608	0.519	0.653	0.656	0.651	0.647	0.541	0.543	0.536	0.546	0.570	0.536	0.485	0.544
Fe^{+3}#	0.110	0.134	0.110	0.092	0.090	0.088	0.128	0.146	0.154	0.113	0.113	0.079	0.141	0.125
Cr+Al	1.632	1.564	1.691	1.772	1.773	1.774	1.575	1.528	1.546	1.635	1.638	1.713	1.566	1.613

Table 3.3. Representative microanalyses of the Cr-spinel with their structural formulas based on 4 oxygen atoms wehrlites of Sawlava ophiolites. (Cr-spinel formulas are calculated calculates with 4 anions and 3 cations).

Sample	Q9						Q43						
Element	1	2	3	4	5	6	1	2	3	4	5	6	7
SiO_2	0.05	0.03	0.09	0.09	0.08	0.08	0.03	0.08	0.09	0.08	2.33	0.06	0.65
TiO_2	0.10	0.08	0.12	0.13	0.08	0.09	0.11	0.07	0.10	0.06	0.06	0.11	0.08
Al_2O_3	26.47	26.23	26.73	26.32	27.02	27.10	26.99	26.44	27.16	28.05	20.06	26.27	29.19
Cr_2O_3	42.34	42.68	42.60	42.03	41.45	41.97	42.10	42.03	42.15	40.67	32.44	42.44	41.65
Fe^2O^3	4.43	4.39	3.41	4.42	4.26	3.20	3.89	4.44	3.61	3.79	16.34	4.38	0.00
FeO	12.55	12.53	12.88	12.74	13.25	14.18	12.93	12.48	13.06	13.80	14.47	12.83	15.57
MnO	0.21	0.19	0.19	0.21	0.20	0.22	0.17	0.20	0.28	0.22	1.22	0.21	0.19
MgO	15.67	15.50	15.58	15.80	15.30	14.65	15.54	15.91	15.36	15.16	14.89	15.54	13.15
CaO	0.00	0.00	0.00	0.02	0.00	0.00	0.00	0.01	0.02	0.01	0.03	0.00	0.05
V_2O_5	0.00	0.00	0.00	0.00	0.00	0.00	0.00	0.00	0.00	0.00	0.00	0.00	0.00
NiO	0.10	0.15	0.12	0.13	0.17	0.23	0.13	0.15	0.12	0.16	0.21	0.14	0.17
ZnO	0.00	0.00	0.00	0.00	0.00	0.00	0.00	0.00	0.00	0.00	0.00	0.00	0.00
Total	100.47	100.35	100.33	100.45	100.38	100.40	100.51	100.37	100.48	99.52	100.41	100.56	100.19
Si	0.001	0.001	0.003	0.003	0.002	0.002	0.001	0.002	0.003	0.002	0.070	0.002	0.019
Ti	0.002	0.002	0.003	0.003	0.002	0.002	0.002	0.002	0.002	0.001	0.001	0.002	0.002
Al	0.914	0.906	0.925	0.910	0.935	0.942	0.932	0.915	0.938	0.972	0.713	0.909	1.017
Cr	0.981	0.991	0.989	0.982	0.962	0.978	0.975	0.980	0.973	0.936	0.773	0.985	0.973
Fe_3	0.098	0.097	0.075	0.097	0.094	0.071	0.086	0.097	0.079	0.084	0.371	0.097	0.000
Fe_2	0.307	0.317	0.316	0.310	0.325	0.350	0.317	0.304	0.326	0.330	0.365	0.315	0.385
Mn	0.005	0.005	0.005	0.005	0.005	0.005	0.004	0.005	0.007	0.005	0.031	0.005	0.005
Mg	0.689	0.677	0.682	0.686	0.670	0.644	0.679	0.691	0.668	0.665	0.669	0.680	0.579
Ca	0.000	0.000	0.000	0.000	0.000	0.000	0.000	0.000	0.001	0.000	0.001	0.000	0.001
Ni	0.002	0.004	0.003	0.003	0.004	0.005	0.003	0.003	0.003	0.004	0.005	0.003	0.004
Tot. cat.	3.000	3.000	3.000	3.000	3.000	3.000	3.000	3.000	3.000	3.000	3.000	3.000	2.984
Cr#	0.518	0.522	0.517	0.519	0.507	0.510	0.511	0.517	0.509	0.491	0.520	0.520	0.489
Fe^{+2}#	0.309	0.319	0.317	0.311	0.327	0.352	0.318	0.306	0.328	0.332	0.353	0.317	0.399
Mg#	0.691	0.681	0.683	0.689	0.673	0.648	0.682	0.694	0.672	0.668	0.647	0.683	0.601
Fe^{+3}#	0.049	0.048	0.037	0.049	0.048	0.035	0.043	0.048	0.039	0.043	0.199	0.048	0.000
Cr+Al	1.895	1.898	1.914	1.892	1.897	1.920	1.907	1.895	1.911	1.909	1.486	1.895	1.989

Table 4. Selected microprobe analyses of olivine samples with their calculated components of peridotites from Sawlava Ophiolites.

Sam	*Min*	*SiO_2*	*TiO_2*	*$Al2O_3$*	*Cr_2O_3*	*FeO*	*MnO*	*MgO*	*CaO*	*Na_2O*	*NiO*	*Total*	*Mg#*	*Fo*	*Fa*
Q43	*1*	*40.28*	*0.03*	*0.00*	*0.05*	*11.25*	*0.15*	*48.05*	*0.1*	*0.00*	*0.3*	*100.2*	*0.88*	*88.30*	*11.6*
	5	*40.21*	*0.02*	*0.02*	*0.04*	*11.11*	*0.21*	*48.32*	*0.11*	*0.00*	*0.21*	*100.2*	*0.88*	*88.40*	*11.40*
	1	*41.24*	*0.00*	*0.03*	*0.02*	*9.15*	*0.15*	*49.27*	*0.19*	*0.00*	*0.39*	*100.44*	*0.90*	*90.50*	*9.40*
	6	*40.78*	*0.01*	*0.00*	*0.03*	*9.20*	*0.17*	*49.7*	*0.18*	*0.00*	*0.42*	*100.49*	*0.90*	*90.40*	*9.40*
	7	*40.64*	*0.00*	*0.03*	*0.00*	*8.82*	*0.17*	*50.29*	*0.17*	*0.05*	*0.42*	*100.59*	*0.91*	*90.90*	*8.90*
Q9	*15*	*40.48*	*0.02*	*0.00*	*0.00*	*8.83*	*0.17*	*50.43*	*0.14*	*0.00*	*0.44*	*100.49*	*0.90*	*90.80*	*9.00*
	18	*40.45*	*0.02*	*0.02*	*0.05*	*8.87*	*0.13*	*50.24*	*0.19*	*0.02*	*0.37*	*100.37*	*0.91*	*90.90*	*9.00*
	20	*40.80*	*0.00*	*0.00*	*0.08*	*8.74*	*0.07*	*49.61*	*0.16*	*0.00*	*0.39*	*99.86*	*0.91*	*90.90*	*9.00*
	22	*40.72*	*0.00*	*0.01*	*0.04*	*8.74*	*0.14*	*50.05*	*0.18*	*0.00*	*0.42*	*100.29*	*0.91*	*91.00*	*8.80*
	1	*40.95*	*0.02*	*0.03*	*0.02*	*9.64*	*0.15*	*49.20*	*0.10*	*0.02*	*0.32*	*100.45*	*0.89*	*89.95*	*9.89*
Q42	*5*	*40.75*	*0.02*	*0.00*	*0.01*	*10.11*	*0.14*	*48.77*	*0.07*	*0.01*	*0.33*	*100.20*	*0.89*	*89.46*	*10.40*
	6	*41.00*	*0.00*	*0.00*	*0.00*	*9.52*	*0.14*	*49.34*	*0.11*	*0.01*	*0.28*	*100.41*	*0.90*	*90.10*	*9.75*
Q11	*8*	*39.81*	*0.04*	*0.00*	*0.03*	*10.69*	*0.17*	*48.20*	*0.09*	*0.07*	*0.30*	*99.41*	*0.89*	*88.60*	*11.3*

Table 5. Selected microprobe analyses of clinopyroxene samples with their calculated components peridotites from Sawlava Ophiolites.

Sample	Min	SiO_2	TiO_2	Al_2O_3	Cr_2O_3	MnO	MgO	CaO	Na_2O	K_2O	FeO	Fe_2O_3	Total	Mg#	Wo	En	Fs
Augite	1	51.82	0.77	3.00	1.40	0.11	17.93	20.53	0.45	0.00	2.79	0.90	99.67	89.80	41.60	51.00	5.80
	2	52.07	0.40	2.21	0.97	0.14	17.96	22.06	0.32	0.01	1.43	1.78	99.54	91.20	44.60	49.40	4.80
	3	51.41	0.51	2.86	1.43	0.16	18.83	19.83	0.43	0.00	0.87	3.07	99.39	90.20	38.70	53.90	5.80
	4	51.53	0.42	3.01	1.35	0.14	17.74	21.42	0.36	0.00	1.12	2.65	99.74	90.00	43.30	49.90	5.50
	5	51.50	1.32	2.97	1.18	0.16	18.30	19.69	0.55	0.00	2.23	1.84	99.73	89.40	40.00	51.80	6.20
	6	51.45	0.35	3.15	1.33	0.13	18.78	20.57	0.31	0.01	0.56	2.96	99.51	91.20	41.00	52.80	5.10
	7	51.45	0.32	2.70	1.13	0.12	18.66	21.88	0.20	0.00	0.40	2.91	99.58	91.60	43.30	51.30	4.70
	8	52.34	0.45	2.91	1.35	0.10	20.06	18.18	0.29	0.01	2.48	2.01	100.21	89.30	36.40	55.90	6.70
	9	51.84	0.52	2.89	1.29	0.11	18.95	19.73	0.43	0.02	1.26	2.81	99.86	89.90	39.60	52.90	5.90
	10	52.00	0.63	2.97	1.37	0.16	18.73	19.97	0.42	0.00	1.69	2.19	100.12	90.10	40.20	52.50	5.80
	11	51.77	0.84	3.21	1.29	0.10	18.88	18.67	0.33	0.00	3.48	0.76	99.33	89.00	38.30	53.90	6.70
	1	52.51	0.24	2.90	1.44	0.17	17.41	21.43	0.32	0.00	3.14	0.00	99.57	90.80	44.02	49.75	5.04
	2	52.57	0.34	1.99	1.22	0.12	18.10	21.76	0.41	0.00	3.02	0.00	99.54	91.43	43.47	50.32	4.72
CEn	1	56.52	0.08	2.03	1.93	0.12	35.76	1.14	0.04	0.00	2.57	0.00	100.19	96.13	2.16	93.94	3.78
	2	56.66	0.11	2.04	1.76	0.10	33.88	1.95	0.11	0.00	2.51	0.00	99.12	96.01	3.80	91.99	3.82

On the ternary diagram of trivalent cations, Cr-Al-Fe^{3+}, Cr-spinel compositions from chromitite and wehrlite plot in podiform mantle chromitite field but those from dunite fall in both podiform and stratiform chromitite fields (Fig. 5a). Fe^{3+} content of chromites hosted in dunites are relatively higher than those related to chromitites (Fig.5a). In Penjween-Walash serpentinites, in Iraq, from core to rim, three stages have been recognized for the formation of spinel: the residual mantle stage, a Cr-rich stage and a third stage which is a

very narrow magnetite rim [22]. In Sawlava serpentinites comparing rim and core composition in ternary diagram (Fe^{3+}-Al-Cr) [32], the composition of chromian spinel is homogenous in chromitite and dunite. Based on the Cr-spinel chemistry, chromitite and dunite formed between deep to shallow mantle. Chromitite formed in deep and dunite formed close to the shallow source (Fig. 5b).

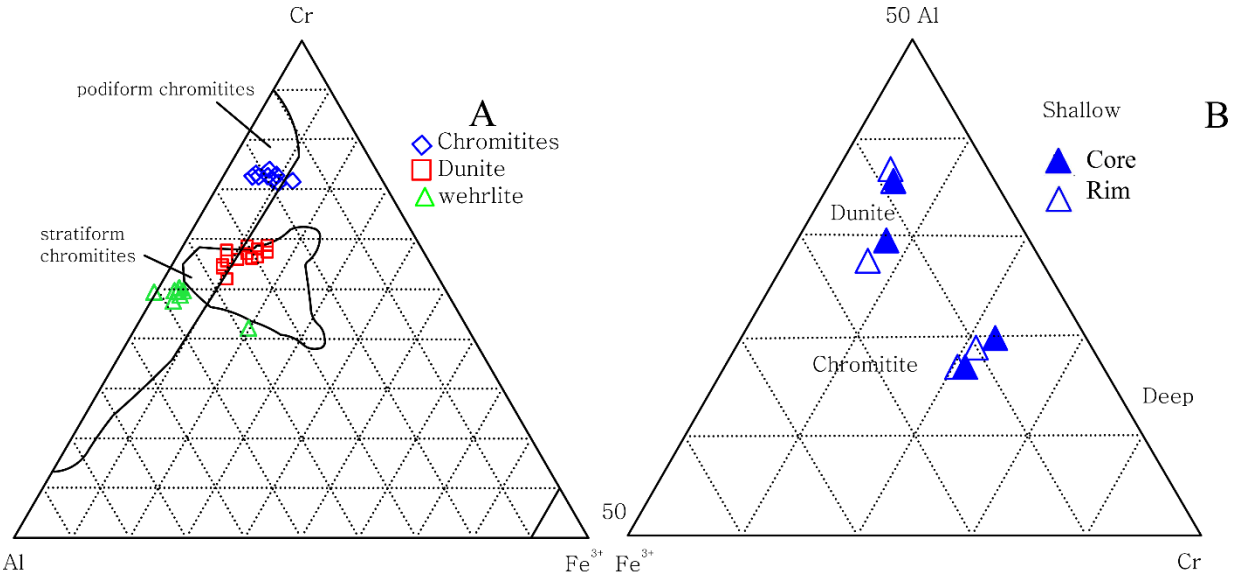

Fig. 5a. The plot of trivalent cations of Cr-spinel in chromitite, dunite and wehrlite from Sawlava ophiolite. Mantle chromitite field after [5] and stratiform chromitite field after [35]. b. A ternary Al-Cr-Fe^{3+} plot [32] for Sawlava Cr-spinels rim and core compositions in the chromitite and dunite. Chromitite and dunite fall between deep and shallow mantle source.

Al-rich and Cr-rich chromites are generated from tholeiitic and high-Mg boninitic magmas, respectively [11, 12 and 36]. In Figure (6), constructed based on Cr# versus Al_2O_3 contents of Cr-spinels, Cr-spinels from wehrlite fall in the high-Al chromitite field; whereas, those from chromitite and dunite plot in high Cr chromitite. In Kermanshah ophiolites, all Cr-spinels from harzburgites and dunites show Cr# and Fe# similar to Cr-spinels from supra-subduction zone (SSZ) peridotites with bononitic characterization [37].

In Sawlava ophiolites, Al_2O_3 and Mg# are increasing from wehrlite to chromitite in the order of chromitite>dunite>wehrlite. Fe^2# in wehrlite is lower than that in dunite and chromitite, also Fe^3# shows the order of dunite>chromitite>wehrlite (Tables 5 and 6). According to the values of Cr_2O_3 (50-57%wt), Sawlava chromitite and dunite can be classified according to the diagram of [9] as high-Cr chromitite type but wehrlite samples fall solely in high-Al chromitite type (Fig. 6). Cr_2O_3 and Al_2O_3 contents of spinels in Kermanshah harzburgites and dunites [37] are very similar to those in Sawlava wehrlitic samples.

As it can be seen from Figure (6), the negative correlation of Al with Cr from Sawlava ultramafic rocks reveals this fact that Al^{3+} is substituted by Cr^{3+} in Cr-spinel structure. In Sawlava chromitite, the low values of TiO_2 (0.08-0.19%wt) is a characteristics of podiform chromitite [38 and 39].

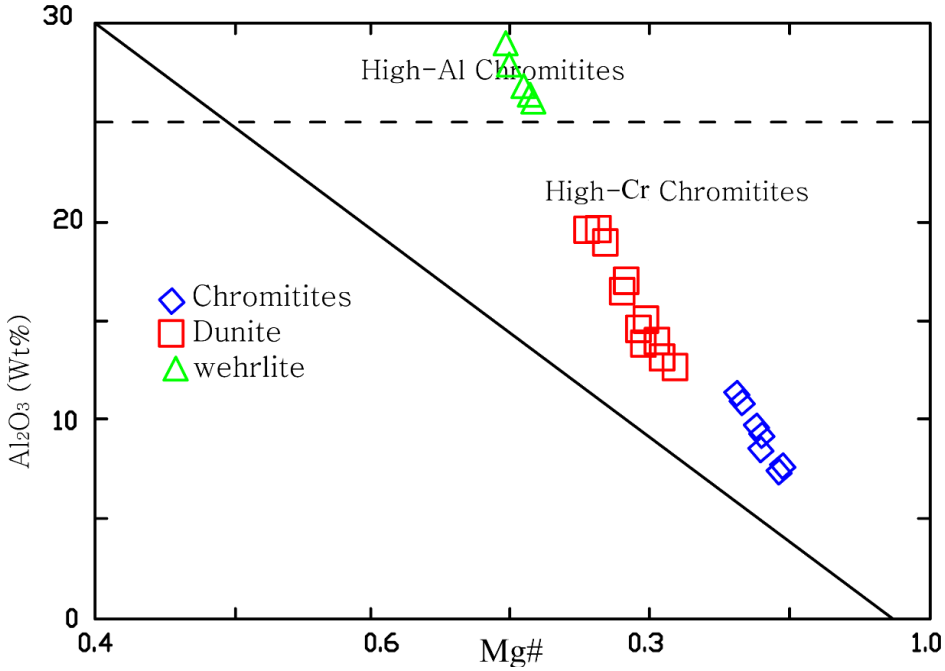

Fig. 6. The position of Sawlava Cr-spinel crystals in Cr# versus Al_2O_3 diagram [9]. Cr-spinel grains from chromitite and dunite plot in high-Cr chromitite field and those from wehrlite fall in high-Al one.

Discussion

Partial melting

In Figure 7, which is a diagram displaying the Mg# in olivine versus Cr# in spinels [2], wehrlite samples plot in the shared fields of abyssal and SSZ peridotites; whereas, dunites and chromitites fall in the SSZ peridotite field. Increasing the $Cr\#_{(Sp)}$ content in peridotites may indicate an increase of partial melting rate [2, 3]. Partial melting rate for Sawlava ophiolites can be estimated from the diagram to be between 25 to 35% in SSZ peridotites field (Fig. 7). Chromitites plot in the SSZ and close to the OSMA (olivine–spinel mantle array) field (Fig. 7) display a good correlation with the bononite fractionation line [3, 40]. In addition, higher partial melting rate of chromitites (>40%) could be related to the bononitic nature of the magma.

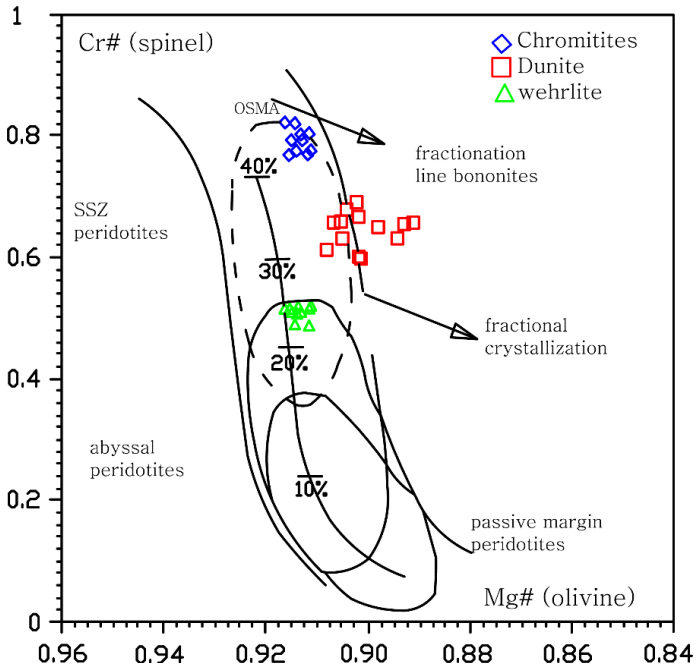

Fig. 7. Cr# in spinel versus Mg# in olivine from peridotites of Sawlava ophiolite. Fields for Cr-spinels occurring in abyssal (and ocean ridge), oceanic SSZ and passive margin peridotites are from [2 and 41]. OSMA field and fractionation line of boninites are from [3, 39].

Nature of magma

Figure 8, created based on the Al_2O_3 versus Cr_2O_3 contents, displays that the chromitite and wehrlite Cr-spinels plot in the podiform chromitite; whereas, dunite Cr-spinels fall in the arc cumulate Cr-spinels field (Fig. 8). As shown earlier in Figure (5a), Cr-spinels in dunite show a mantle origin.

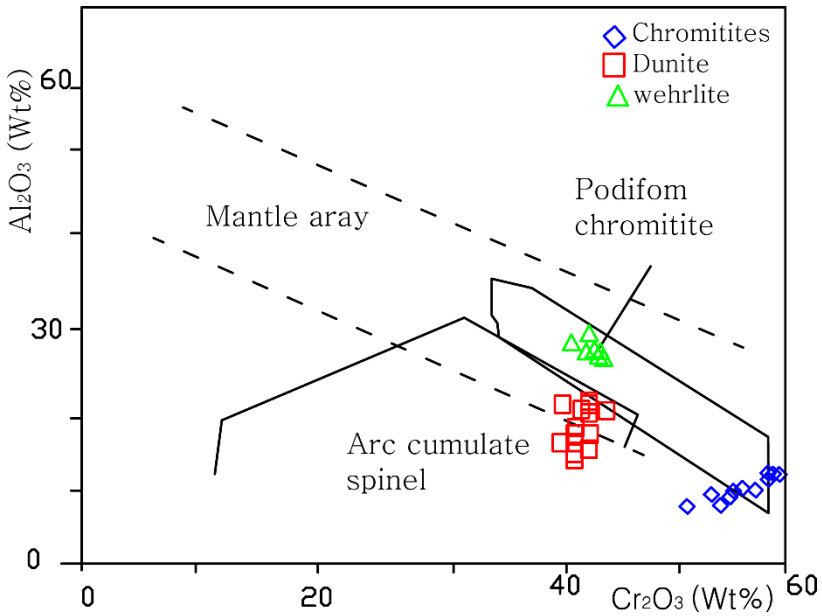

Fig. 8. Al_2O_3 versus Cr_2O_3 contents in the chromitites are used to determine their origin and type. Spinel fields are from [42, 43 and 44] and chromite types are from [45]. Chromitite and wherlite Cr-spinels plotted in podiform field but dunites samples fall in arc cumulate spinel. Also all samples plot in mantle array field.

The chemical composition of Cr-spinel is used to constrain the chemistry of the parental melt [46]. The Al_2O_3 content of the parental melt can be calculated, using the equation of [47], that is:

$$(Al_2O_3)_{spinel} = 0{\cdot}035(Al_2O_3)^{2.42}_{melt} \ (Al_2O_3 \text{ in wt\%})$$

The Al_2O_3 content of the parental melt is 10.80 wt% for the chromitite (Table 6). Using the chemistry of Cr-spinels, the Al_2O_3 contents calculated for dunite and wehrlite are 12.50 and 16.88 wt%, respectively. The FeO/MgO ratio in the parental magma can be estimated from the FeO/MgO ratio of Cr-spinel using the empirical formulation of [46] that is:

$$\text{Ln. } (FeO/MgO)_{Spinel} = 0{\cdot}47 - 1{\cdot}07XAl_{Spinel} + 0{\cdot}64XFe^{3+}_{Spinel} + \ln(FeO/MgO)_{melt} \text{ where}$$

$$XAl_{Spinel} = Al/(Al + Cr + Fe^{3+}) \text{ and } XFe^{3+}_{Spinel} = Fe^{3+}/(Al + Cr + Fe^{3+})$$

The FeO/MgO values estimated in range of 1.20-2.16 for the chromitite, 1.41-2.79 for dunite and 1.03-1.95 for wehrlite (Table 6). Although the host rocks (dunite and wehrlite) indicate an equivocal nature for the parental melts, the chemistry of chromitite shows clearly a boninitic composition for the parental melt. The plot of TiO_2 wt% versus Cr# shows that the Cr-spinels in chromitite plot in the boninitic field and the Cr-spinels in wehrlite fall in the depleted peridotite fields, whereas the Cr-spinels in dunite plot in both the depleted and MORB peridotite fields (Fig. 9). Re-equilibration of the Fe and Mg cations between silicates and spinel may change these values considerably [48].

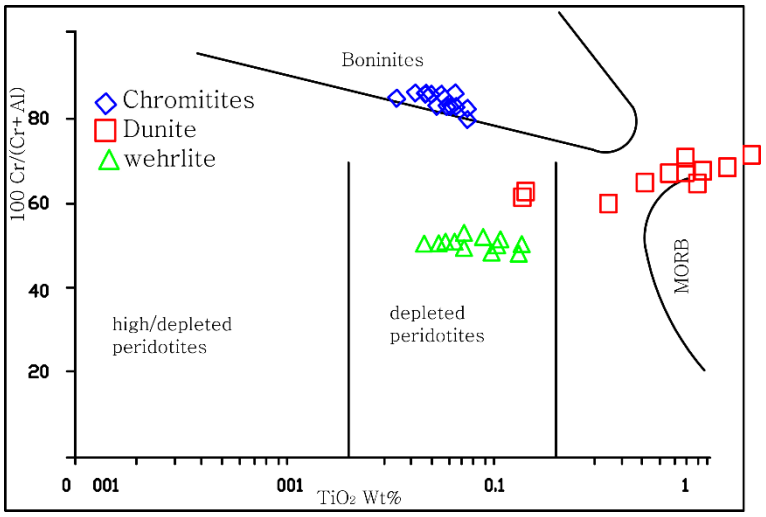

Fig 9. TiO_2 contents (wt%) versus Cr# in Cr-spinels and positions of Cr-spinels from Sawlava ophiolite [49].

Table 6 - Al_2O_3 content (wt %) and FeO/MgO ratios of the parental melt and calculated degree of partial melting (F). The formula of [49] was used for estimating the degree of partial melting of the source materials: F% = 10 ln (Cr# spinel) +24. Chromitite lenses are from Nain ophiolite [48].

component	*chromitite*	*dunite*	*wehrlite*	*chromitite lenses (Nain)*
Al_2O_3 in Spinel	*7.36-11.52*	*12.52-19.79*	*20.60-29.19*	*13.78-14.87*
Al_2O_3 in Melt	*10.80*	*12.50*	*16.86*	*11.58-11.95*
FeO/MgO	*1.20-2.16*	*1.41-2.79*	*1.03-1.95*	*0.83-0.84*
F%	*21.33-22.02*	*18.60-20.26*	*16.87-17.50*	*20.52-20.72*

Table 7 - Comparison of Cr-spinel compositions from Sawlava complex with Cr-spinels from other known tectonic settings (data from [50] adopted from [47].

Deposite	*$Mg/Mg+Fe^{2+}$*	*Cr/Cr+Al*	*Cr/Fe_t*	*Fe^{3+}/Fe^{2+}*	*Ti^{4+} per 4 O*
Sawlava chromitite	*0.53-0.72*	*0.77-0.82*	*2.22-2.38*	*0.23-0.76*	*0.002-0.004*
Sawlava dunite	*0.48-0.65*	*0.58-0.69*	*1.28-2.05*	*0.30-0.58*	*0.023-0.103*
Sawlava wehrlite	*0.60-0.69*	*0.49-0.52*	*2.26-2.52*	*0.20-0.32*	*0.001-0.003*
Selukwe	*0.68-0.70*	*0.69-0.73*	*2.70-4.80*	*0.00-0.25*	*0.060-0.100*
Bushveld	*0.24-0.58*	*0.60-0.75*	*0.95-3.0*	*0.16-1.12*	*0.130-1.060*
Great Dyke	*0.36-0.67*	*0.70-0.80*	*2.10-3.90*	*0.14-0.26*	*0.020-0.480*
Cyprus	*0.47-0.74*	*0.42-0.84*	*2.10-3.80*	*0.02-0.48*	*0.020-0.040*
Oman	*0.47-0.71*	*0.11-0.80*	*0.80-3.90*	*0.00-0.24*	*0.010-0.040*
Nain Chromite Patch	*0.58-0.63*	*0.50-0.68*	*2.60-3.30*	*0.00-0.23*	*0.003-0.008*
Nain chromite lenses	*0.68-0.70*	*0.68-0.73*	*3.13-3.46*	*0.26-0.30*	*0.005-0.007*

Geotectonic setting

Cr/Fe_{total} ratio of Cr-spinels is 2.22 to 2.38 (Table 6) and plot in the ophiolite-related Cr-spinels field in the Cr-Al-Fe^{3+} diagram (Fig. 5A) and they also plot in the field of podiform chromite originated from the mantle, in the Al_2O_3 versus Cr_2O_3 diagram (Fig. 8). The Mg# versus Cr# diagram for spinel can be used to attribute peridotites to either Alpine I-type peridotites [2], abyssal peridotites, fore-arc peridotites [52] and back arc peridotites [53]. In this diagram, the chromitite samples plot in the Alpine-type peridotite field, dunite and wehrlite in the fore-arc peridotite and wehrlite plot in the abyssal peridotite (Fig. 10). Note all studied Cr-spinels define Alpine-type.

[54] Suggested that the Fe^{2+}/Fe^{3+} ratio (calculated based on stoichiometry) and TiO_2 content of spinel could be used to characterize supra-subduction zone (SSZ) and MOR type peridotites. Al_2O_3 content versus TiO_2 and Fe^{2+}/Fe^{3+} diagrams (Fig. 11) show that the investigated Cr-spinels from wehrlite plot in the transitional field of MOR peridotites to SSZ peridotites and SSZ (i.e. marginal basin) peridotites. For chromite from chromitites, the Al_2O_3 liquid values and FeO/MgO liquid ratios are estimated to be 10.80 wt%

and 1.20-2.16, respectively (Table. 6). These values are comparable to the Nain chromitite in Iran [48] and show a boninitic source for the rocks (Table 7). The boninitic magmatism is restricted to supra-subduction zones [55, 56 and 57]. Sawlava peridotite is almost similar in spinel chemistry to the harzburgite most commonly found from the Oman ophiolite [58 and 59] (Fig. 12). However, in Sawlawa ophiolites Cr-spinel related to lherzolite, similar to the Oman ophiolites (Cr# of spinel < 0.3) [60 and 61] are not present (Fig. 12).

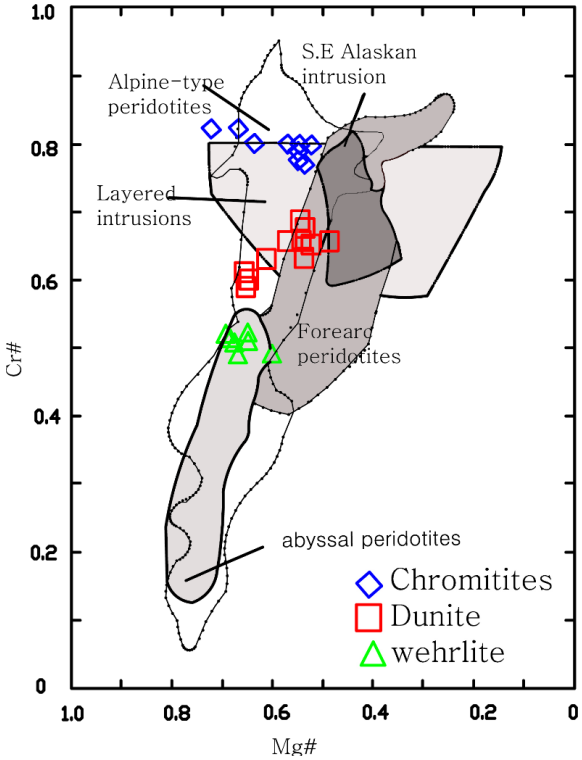

Fig.10. Cr-spinels Mg# versus Cr# diagram: Field of Alpine I-type peridotites was taken from [2], fore-arc and abyssal peridotites after [52], back arc peridotites from [53]. Chromitite samples plot in the abyssal peridotite and dunite; whereas, wehrlite fall in the Alpine-type peridotite. Dunite also plot in the fore-arc peridotite.

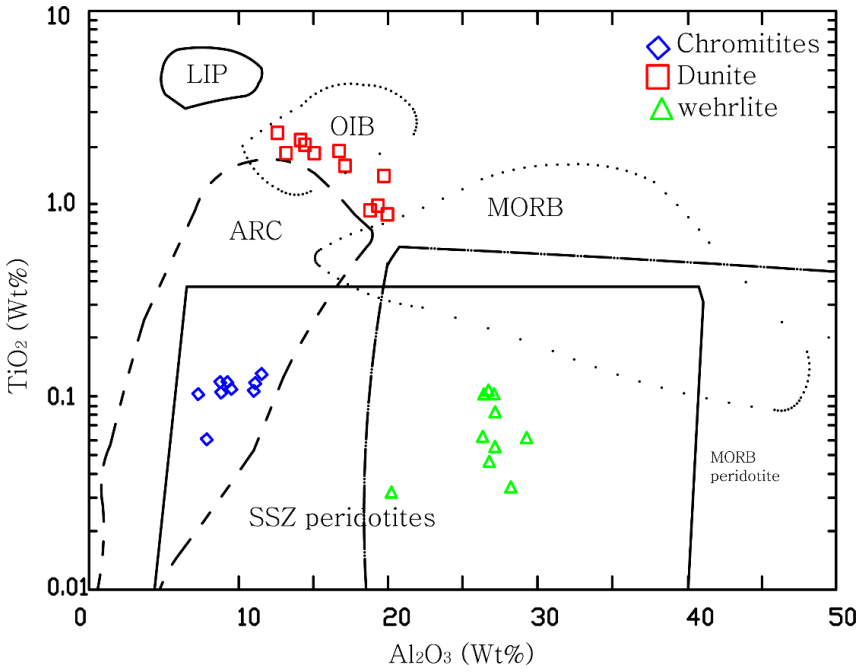

Fig. 11. Al_2O_3 versus Fe^{2+}/Fe^{3+} tectonic discrimination diagram. Fields of supra-subduction zone (SSZ) peridotites and MOR peridotites are from [54].

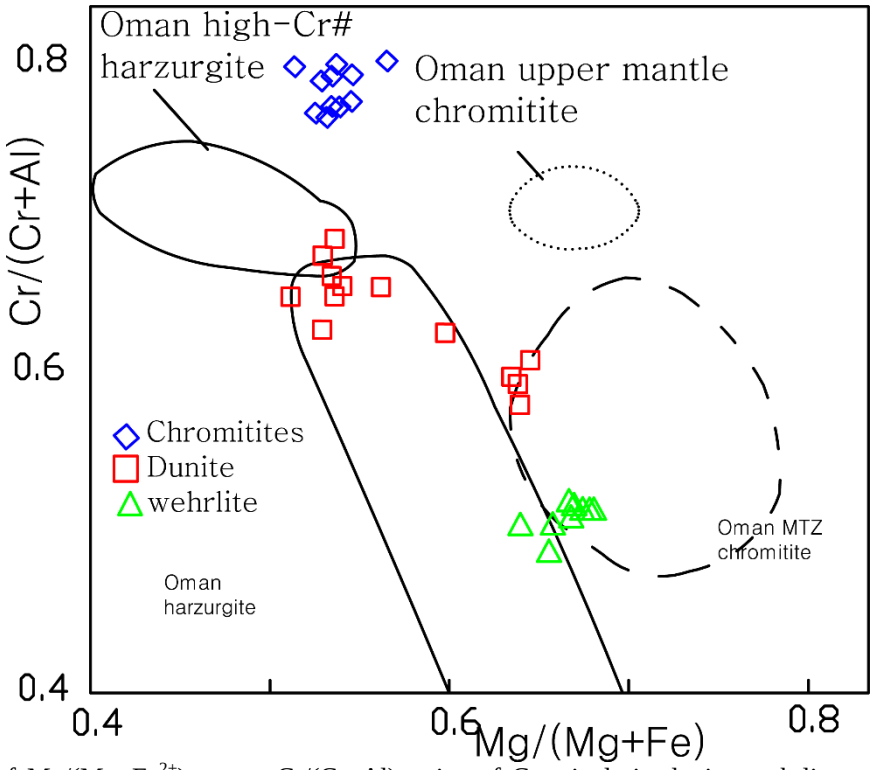

Fig. 12 The plot of $Mg/(Mg+Fe^{2+})$ versus Cr/(Cr+Al) ratios of Cr-spinels in dunite, wehrlite and chromitites from Sawlava. Compositional ranges for Cr-spinels in chromitites from the upper mantle and the Moho transition zone (MTZ) from the Oman ophiolite [7 and 46] are shown for comparison. The ranges for ordinary harzburgites and highly depleted harzburgites from the Oman ophiolite are after [52 and 59], respectively. The Cr# from Sawlava chromitite is higher than that of all Cr-spinel in Oman ophiolite. The Sawlava dunite is almost transitional between MTZ and high and low harzburgite from the Oman ophiolite but its trend is similar to the low Cr# Oman harzburgite. Sawlava wehrlites also plot between MTZ and low Cr# harzburgite.

Regional application

The peridotites of Zagros ophiolite have high Cr# spinel compositions that mostly plot in the fore-arc field [62]. Figures 12 shows the tectonic affinities of the study samples are within the fore-arc setting of peridotite. The similarities between Cr# spinel compositions of Sawlava samples and the peridotites of Zagros ophiolite validate the conclusion that a broad and continuous tract of fore-arc lithosphere was created during the late Cretaceous [62].

Also from Kurdistan region in Iraq, the tectonic affinity based on the chemical characteristics of primary Cr-spinels is within the fore-arc setting of peridotite rootlets. The evidence confirms the suggestion that fore-arc serpentinites contributed to exhumation of overlying rocks during active subduction starting in the late Maastrichtian and during late pre-collisional activity [22] and Sawlava is a small part of the vast ophiolitic complexes which formed during the closure of the Neo- Tethys and Zagros orogeny.

All Cr-spinels from harzburgitic rocks and dunites in Kermanshah ophiolites show Cr# and Fe# similar to those of Cr-spinels from supra-subduction zone (SSZ) peridotites; also REE modeling shows that they may represent a residual mantle after 25-30% removal of boninitic-type melts in an intra-oceanic arc setting [37].

[23] Believe that it is possible that the Oskul (west of Sawlava area) and gabbroic bodies originated from the back-arc basin rather than a normal island arc. The existence of some dismembered deformed peridotites with the basaltic rocks in the northern Kamyaran suggest that this complex is some part of supra subduction zone ophiolite which was generated from 54 to 36 Ma in the Neotethyan ocean and compressed between the Arabian and Iranian plates in the late Miocene or younger.

As stated above, the age of Zagros ophiolites are Cretaceous [63, 64] however, recent study by [23] on Kamyaran ophiolite, which is the closest ophiolite to the study area, has shown an Eocene age (54 Ma for

basalts and 37 Ma for gabbros), Therefore it seems that the Sawlava ophiolite cannot be of Cretaceous age. The different ages probably indicate different geodynamic environment for the Kurdistan ophiolite formation. Field evidences indicate that ophiolites were formed near the Sanandaj-Sirjan zone edge; whereas, geochemical data in various tectonic diagrams display a supra-subduction zone environment for the generation of the ophiolites.

Conclusion

Cr-spinel is the main useful mineral to understand primary petrological characteristics of highly altered ophiolitic ultramafic rocks in Sawlava ophiolitic complex.

Cr# from Sawlava ophiolitie Cr-spinels especially in chromitite is high and indicates the boninitic nature of the parental melts.

Dunite displays the SSZ peridotite characterization despite the fact that Cr-spinels in wehrlite show the MOR characterization (abyssal peridotite), Although the host rocks (dunite and wehrlite) do not indicate an unequivocal nature for the parental melts using the calculations mentioned above, the chemistry of chromitite shows a boninitic composition for the parental melt and this fact is an important case to the ocean arc generation of magma source for peridotites from Sawlava ophiolites.

In spite of the high content of Al and Cr# in perioditite Cr-spinels and low value of Ti, Sawlava complex source belongs to a mantle wedge with the high degree of partial melting. These characteristics suggest a fore-arc basin setting for the generation of the chromitite for Sawlava ophiolites. Sawlava peridotites and related podiform chromitites along the Zagros suture formed on Neo-Thetys Ocean and the results obtained from this study could be used for ophiolitic complexes in other parts of the Zagros orogen in order to evaluate a unique model for the source and evolution of the magmatism in this part of the Alpine orogen.

Acknowledgment

We would like to thank E. Saccani from Università di Ferrara, Italy and Kh. Allahyari from Shahid Beheshti University, Iran for their support with the EPMA analyses.

Reference

[1] Irvine T.N. *"Cr-spinel as a petrogenetic indicator; Part 2, petrologic applications*". Canadian Journal of Earth Sciences, 4, 71_103. 1967.

[2] Dick H.J.B. and Bullen T. *"Chromian spinel as a petrogenetic indicator in abyssal and alpine-type peridotites and spatially associated lavas".* Contributions to Mineralogy and Petrology, 86: 54-76. 1984.

[3] Arai S. *"Characterization of spinel peridotites by olivine-spinel compositional relationships: Review and interpretation".* Chemical Geology, 113, 191_204. 1994a.

[4] Barnes S.J. and Roeder P.L. *"The range of spinel compositions in terrestrial mafic and ultramafic rocks*". Journal of Petrology, 42, 2279-2302. 2001.

[5] Arai S., Shimizu Y., Ismail S.A. and Ahmad A.H. *"Low-T formation of high-Cr spinel with apparently primary chemical characteristics within podiform chromitite from Rayat, northeastern Iraq"*. Mineralogical Magazine, Vol. 70(5), pp. 499–508. 2007.

[6] Barnes S.J. *"Chromite in komatiites, II. Modification during greenschist to mid-amphibolite facies metamorphism".* Journal of Petrology, 41, 387-409. 2000.

[7] Ahmed A.H., Arai S. and Attia, A.K. *"Petrological characteristics of the Pan African podiform chromitites and associated peridotites of the Proterozoic ophiolite complexes, Egypt".* Mineralium Deposita, 36, 72-84. 2001.

[8] Abzalov M.Z. "*Chrome-spinels in gabbro wehrlite intrusions of the Pechenga area, Kola Peninsula, Russia: emphasis on alteration features*". Lithos, 43, 109-134. 1998.

[9] Leblanc M. and Violette J.F. *"Distribution of Al-rich and Cr-rich chromite pods in ophiolites".* Economic Geology 78: 293-301. 1983.

[10] Zhou M.F. and Robinson P.T. *"High-Cr and high-Al chromitites western China: relationship to partial melting and melt/rock interaction in the upper mantle"*. International Geological Reviews 36, 678-686. 1994.
[11] Hock M., Friedrich G., Pluer, W.L. and Wichowski A. *"Refractory and metallurgical-type chromite ores. Zarnbale ophiolite, Luzon, Phillipines*". Mineralium Deposita. vol. 21 . pp. 190-199. 1986.
[12] Yumul G.P., Jr. and Balce U.K. *"Supra-subduction zone ophiolites as favorable hosts for chromitite, platinum and massive sulfide deposits"*. Journal of Southeast Asian Earth Sciences, 10, 65-79. 1994.
[13] Lachance G.R. and Trail R.J. *"Practical solution to the matrix problem in X-ray analysis*". Canadian Spectroscopy 11: 43-48. 1966.
[14] Pouchou J.L. and Pichoir F. *"PAP (pZ) procedure for improved quantitative microanalysis, In: J.T. Armstrong (Ed.), Microbeam analysis"*. San Francisco Press, San Francisco, p. 104-106. 1985.
[15] Droop G.T.R. *"A general equation for estimating Fe^{3+} concentrations in ferromagnesian silicates and oxides from microprobe analyses, using stoichiometric"* Contributions to Mineralogy and Petrology, 51: 431-435. 1987.
[16] Berberian, M. and King G.C.P. *"Toward a paleogeography and tectonic evolution of Iran"*. Canadian Journal of Earth Science 18: 210–265. 1981.
[17] Agard P., Jolivet L., Vrielynck B., Burov E. and Monié, P., "*Plate acceleration: The obduction trigger?*" Earth and Planetary Science Letters 258: 428–441. 2007.
[18] Agard P., Omrani J., Jolivet L. and Mouthereau F. *"Convergence history across Zagros (Iran): constraints from collisional and earlier deformation"*. Institute Journal of Earth Science (Geol. Rundsch.) 95: 401- 419. 2005.
[19] Ghazi A.M. and Hassanipak A.A. *"Geochemistry of sub-alkaline and alkaline extrusive from Kermanshah Ophiolite, Zagros suture zone, western Iran: implications for Tethyan plate tectonics"*. Journal of Asian Earth Science 17 (3): 319-332. 1999.
[20] Nadimi A., "*Mantle flow patterns at the Neyriz Paleo – spreading centre, Iran"*. Earth and Planetary Science Letters 203: 93-104. 2002.
[21] Sarkarinejad K. *"Petrology and tectonic setting of the Neyriz ophiolite, southeast Iran. In: Ishiwatari, A., Malpas, J. and Ishizuka, H. (Eds.), Circum-Pacific Ophiolites"*, Proceedings of 29th International Geological Congress, Part D, 221-234. 2005.
[22] Aswad J.A.Kh., Nabaz Aziz R.H. and Koyi H.A. *"Cr-spinel compositions in serpentinites, and their implications for the petrotectonic history of the Zagros Suture Zone, Kurdistan Region, Iraq"*. Geological Magazine. 2011.
[23] Azizi H., Tanaka T., Asahara Y., Chung S. L. and Zarrinkoub M. H. *"Discrimination of the age and tectonic setting for magmatic rocks along the Zagros thrust zone, northwest Iran, using the zircon U–Pb age and Sr–Nd isotope"*. Journal of Geodynamics 52: 304– 320. 2011.
[24] Dilek Y. and Furnes H. *"Structure and geochemistry of Tethyan ophiolites and their petrogenesis in subduction rollback systems"*. Lithos 113: 1-20. 2009
[25] Khalatbari-Jafari M., Juteau T. and Cotton, J. *"Petrological and geochemical study of the Late Cretaceous ophiolites of Khoy (NW Iran), and related geological formations"*. Journal of Asian Earth Science 27 (4): 465-502. 2006.
[26] Alavi, M., *"Tectonics of the Zagros orogenic belt of Iran; new data and interpretations*". Tectonophysics 229, 211–238. 1994.
[27] Sabzehai M., Gourabjiri A. and Eslamdoust F. *"1/100000 Geological map of the Paveh and east of Paveh"*. Geological survey of Iran. 2009.
[28] Whitney, D. L. and Evans, B.W. *"Abbreviations for names of rock-forming minerals"*. American Mineralogist, Volume 95, 185–187. 2010.
[29] Snow, J.E., Dick, H.J.B., Pervasive magnesium loss by marine weathering of peridotite. Geochimica Et Cosmochimica Acta 59 (20), 4219–4235. 1995.

[30] Casey J. *"Comparison of major-and trace-element geochemistry of abyssal peridotites and mafic plutonic rocks with basalts from the Mark Region of Mid-Atlantic Ridge"*. Proc. ODP. Sci. Res., 153: 181-241. 1997.

[31] Ismail S. A., Carr P. F. & Mirza T. *"Platinum-group elements geochemistry in podiform chromitites and associated peridotites of the Mawat ophiolite, northeastern Iraq"*. Journal of Asian Earth Sciences, 37 (1), 31-41. 2010.

[32] Rollinson H. *"The geochemistry of mantle chromitites from the northern part of the Oman ophiolite: inferred parental melt compositions"*. Contributions to mineralogy and petrology, 156:273–288. 2008.

[33] McDonough W.F. and Sun S.S. *"The composition of the Earth"*. Chem. Geol., 120: 223-253.

[34] Medaris Jr. G., Wang H., Jelinek E., Mihaljevič M. and Jakeš P. *"Characteristics and origins of diverse Variscan peridotites in the Gfˇhl Nappe, Bohemian Massif, Czech Republic"*. Lithos, 82: 1-23. 2005.

[35] Proenza J.A., Zaccarini F., Lewis J.F., Longo F. and Garuti G. *"Chromian spinel composition and the platinum-group minerals of the PGE-rich Lomapegvera chromitites, Loma Caribe peridotite"*. Donimican Republiccanadian journal of mineralogy, 45: 631-648. 2007.

[36] Robinson P.T., Zhou M.F., Malpas J. and Bai W.J. *"Podiform Chromitites: Their composition, origin and environment of formation"*. Episodes 20, 247-252. 1997.

[37] Allahyari K., Sacanni E., Pourmoafi M., Beccalova L. and Masoudi, F. *"Petrology of mantle peridotites and intrusive mafic rocks from the Kermanshah ophiolitic complex (Zagros belt, Iran): implication for the geodynamic evolution of the Neo-Tethyan oceanic branch between Arabia and Iran"*. Ofioliti 35: 71–90. 2010

[38] Ferrario A. and Garuti G. *"Platinum-group mineral inclusions in chromitites of the mafic ultramafic complex (Ivrea-Zone, Italy)"*. Mineralogy and Petrology 41:125-143. 1988.

[39] Zaccarini F., Pushkarev E. and Garuti G. *"Plutinum-group element mineralogy and geochemistry of chromitite of the Kluchevskoy ophiolite complex, central Urals (Russia)"*. Ore geology reviews, 33, 20-30. 2001.

[40] Arai S. *"Compositional variation of olivine chromian spinel in Mg-rich magmas as a guide to their residual spinel peridotites"*. Journal of Volcanology and Geothermal Research, 59, 279_294. 1994b.

[41] Pearce J.A., Barker P.F., Edwards S.J., Parkinson I.J. and Leat P.T. *"Geochemistry and tectonic significance of peridotites from the South Sandwich arc-basin system, South Atlantic"*. Contributions to Mineralogy and Petrology 139, 36–53. 2000.

[42] Conrad W.K. and Kay R.W. *"Ultramafic and mafic inclusions from Adak Island: crystallization history and implications for the nature of primary magmas and crustal evolution in the Aleutian arc"*. Journal of Petrology 25, 88–125. 1984.

[43] Haggerty S.E., *"Upper mantle opaque mineral stratigraphy and the genesis of metasomaties and alkali-rich melts"*. J. Geol. Soc. Australia, 14: 687-699. 1988.

[44] Kepezhinskas P.K., Defant M.J. and Drummond M.S. *"Na metasomatism in the island-arc mantle by slab melt-peridotite interaction: Evidence from mantle xenoliths in the north Kamchatka arc"*. Journal of Petrology 36, 1505–1527. 1995.

[45] Bonavia F.F., Diella V. and Ferrario A. *"Precambrian podiform chromitites from Kenticha Hill, Southern Ethiopia"*. Econ. Geol., 88: 198-202. 1993.

[46] Augé T. *"Chromite deposits in the northern Oman ophiolite: mineralogical constraints"*. Mineralium Deposita 22, 1–10. 1987.

[47] Maurel C. and Maurel P. *"Tude expérimentale de la solubilité du chrome dans les bains silicatés basiques et sa distribution entre liquide et minéraux coexistants: conditions d'existence du spinelle chromifère"*. Bulletin of Minéralogy, 105: 640-647. 1982.

[48] Ghazi J.M., Moazzen M., Rahghoshay M. and Shafaii Moghadam H. *"The geodynamic setting of the Nain ophiolites, central Iran: evidence from chromian spinels in the chromitites, and associated rocks"*. Ofioliti, 36 (1), 59-76 59. 2011.

[49] Ferrario A. and Garuti G. *"Platinum-group mineral inclusions in chromitites of the mafic ultramafic complex (Ivrea-Zone, Italy)"*. Mineralogy and Petrology 41:125-143. 1988.

Hellebrand E., Snow J.E., Dick H.J.B. and Hofmann A.W. *"Coupled major and trace elements as indicators of the extent of melting in mid-ocean ridge peridotites"*. Nature, 410 (6829): 677-681. 2001.

[51] Stowe C.W. *"Compositions and tectonic settings of chromite deposits through time"*. Econ. Geol., 89: 528-546. 1994.

[52] Tamura A. and Arai S. "*Harzburgite–dunite–orthopyroxenite suite as a record of supra-subduction zone setting for the Oman ophiolite mantle"*. Lithos 90, 43–56. 2006.

[53] Monnier C., Girardeau J., Maury R. and Cotten J. *"Back-arc basin origin for the East Sulawesi ophiolite (eastern Indonesia)"*. Geology 23, 851–854. 1995.

[54] Kamenetsky V.S., Crawford A.J. and Meffre S. *"Factors controlling chemistry of magmatic spinel: an empirical study of associated olivine, Cr-spinel and melt inclusions from primitive rocks"*. Journal of Petrology 42:655–671. 2001.

[55] Pearce J.A., van der Laan S.R., Arculus R.J., Murton B.J., Ishii T., Peate D.W., Parkinson I.J. *"Boninite and harzburgite from LEG 125 (Bonin–Mriana Forearc): a case study of magma genesis during the initial stages of subduction. In: Fryer, P., Pearce, J.A., Stokking, L.B. (Eds.), Proceedings of the Ocean Drilling Program, Scientific Results, vol. 125. Ocean Drilling Program"*. College Station, TX, pp. 623–657. 1992.

[56] Pearce J.A., Barker P.F., Edwards S.J., Parkinson I.J. and Leat P.T. *"Geochemistry and tectonic significance of peridotites from the South Sandwich arc-basin system, South Atlantic"*. Contributions to Mineralogy and Petrology 139, 36–53. 2000.

[57] Taylor R.N., Nesbitt R.W., Vidal P., Harmon R.S., Auvray B. and Croudace I.W. *"Mineralogy, chemistry, and genesis of the boninite series volcanics, Chichijima, Bonin Islands, Japan"*. Journal of Petrology 35, 577–617. 1994.

[58] Kadoshima K. *"Petrological characteristics of the mantle section of the northern Oman and Lizard ophiolites: an approach from in-situ rocks and detrital chromian spinel"*. PhD. thesis, [1] Kanazawa University, Kanazawa. 2002.

[59] Lemee L., Giradeau J. and Monnier C. *"Mantle segmentation along the Oman ophiolite fossil midocean ridge"*. Nature 432, 167–72. 2004.

[60] Lippard S.J., Shelton A.W. and Gass I.G. *"The ophiolite of northern Oman"*. Geol Soc Mem vol 11. 1986.

[61] Takazwa E., Okayasu T. and Satoch K. *"Geochemistry and origin of the basal lherzolites from the northern Oman ophiolite (northern Fizh block)"*. Geochemistry, Geophysics, Geosystems 4, 1021. 2003.

[62] Shafaii Moghadam H. and Stern R. J. *"Geodynamic evolution of Upper Cretaceous Zagros ophiolites: formation of oceanic lithosphere above a nascent subduction zone"*. Geological Magazine 148: 762–801. 2011.

[63] Delaloye, M., Desmons, J. *"Ophiolites and mélange terranes in Iran: a geochronological study and its paleotectonic implications"*. Tectonophysics: 68, 83–111. 1980.

[64] Davoudian, A.R., Genser, J., Dachs, E., and Shabanian, N. *"Petrology of eclogites from north of Shahrekord, Sanandaj-Sirjan zone, Iran"*. Mineralogy and Petrology, March Volume 92, Issue 3-4, pp 393-413. 2008.